Supplementary Information:

Cooperative wrapping of nanoparticles of various sizes and shapes by lipid membrane

Kai Xiong,[a] Jiayin Zhao,[b] Daowen Yang,[c] Qingwen Cheng,[d] Jiuling Wang*[ef] and Hongbing Ji*[g]

[a] Beijing Municipal Key Laboratory of Resource Environment and GIS, College of Resource Environment and Tourism, Capital Normal University, Beijing 100048, China

[b] College of Environmental Sciences and Engineering, Peking University, Beijing 100871, China

[c] TCM Lung Disease Department, China-Japan Friendship Hospital, Beijing 100029, China

[d] China Aerospsce Science & Industry CORP, Beijing 100048, China

[e] LNM, Institute of Mechanics, Chinese Academy of Sciences, Beijing 100190, China

[f] School of Engineering Sciences, University of Chinese Academy of Sciences, Beijing 100049, China

[g] School of Energy and Environmental Engineering, University of Science and Technology Beijing, Beijing 100083, China

Corresponding authors: wangjiuling2014@gmail.com, ji.hongbing@hotmail.com

Interaction between different beads

The follow potentials are used in the simulations to describe the interaction between different beads:[1, 2]

$$U_{LJ}(r) = 4\alpha\varepsilon\left[\left(\frac{b}{r}\right)^{12} - \left(\frac{b}{r}\right)^{6}\right], \left(0 < r < r_{cut} = 2.5b\right), \quad (1)$$

$$U_{WCA}(r) = 4\varepsilon\left[\left(\frac{b}{r}\right)^{12} - \left(\frac{b}{r}\right)^{6} + \frac{1}{4}\right], \left(0 < r < r_{cut} = 2^{1/6}b\right), \quad (2)$$

$$U_{COS}(r) = \begin{cases} -\varepsilon + U_{WCA}(r), \left(r < r_{cut} = 2^{1/6}b\right) \\ -\varepsilon cos^{2}\dfrac{\pi(r - r_{cut})}{2w}, \left(r_{cut} \le r \le r_{cut} + w\right) \end{cases}, \quad (3)$$

$$U_{FENE}(r) = -\frac{1}{2}k_{FENE}r_{\infty}^{2}ln\left(1 - \frac{r^{2}}{r_{\infty}^{2}}\right), \left(0 < r < r_{\infty}\right). \quad (4)$$

In the simulations, ε and σ are used as the units of energy and length. Comparing to a typical membrane thickness of 5 nm, the bead diameter, σ, is about 1 nm. The parameter ε can be deduced from the temperature, which is set as $k_BT = 1.1\varepsilon$. The neighboring beads are connected by FENE bond with $k_{FENE} = 30\varepsilon$ and $r_{\infty} = 1.5\sigma$, the head bead and the second tail bead are also connected by a harmonic spring with equilibrium bond length $r_0 = 4\sigma$ and force constant $k_{bend} = 10\varepsilon/\sigma^2$. The interactions between NPs and

membrane are listed in Table S1.

Table S1: Interaction parameters for different particle types

bead type	bead type	interaction	parameters
lipid head	lipid head	WCA	b = 0.95σ
lipid head	lipid tail	WCA	b = 0.95σ
lipid tail	lipid tail	COS	b =σ, w= 1.7σ
lipid head	NP	LJ	b =σ, α=1.0
lipid tail	NP	WCA	b =σ
NP	NP	WCA	b =σ

Lipid membrane tension

The membrane tension is calculated according to:[3]

$$\sigma_t = \left\langle l_z \times \left(p_{zz} - \frac{1}{2}(p_{xx} + p_{yy}) \right) \right\rangle, \quad (5)$$

where σ_t is the surface tension, p_{xx} and p_{yy} are tangential components of the pressure tensor, p_{zz} is the normal component and l_z is the thickness of the lipid bilayer. The calculated membrane tension is about $1.9 \times 10^{-2}\, pN/nm$. In addition, due to the relatively large size of our membrane patch, the membrane would collapse (shrink significantly) after a long period of simulation if we set the barostat pressure at zero.

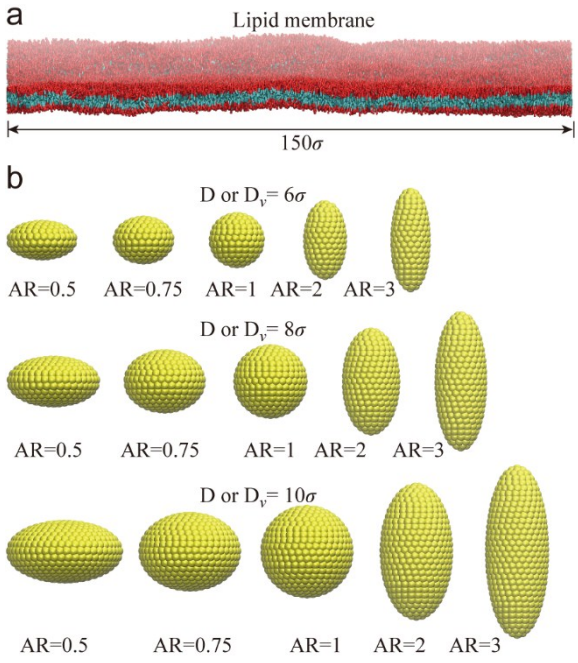

Fig. S1 (a) Illustration of the lipid membrane used in our simulations. (b) All NPs with different

sizes and aspect ratios used in our simulations.

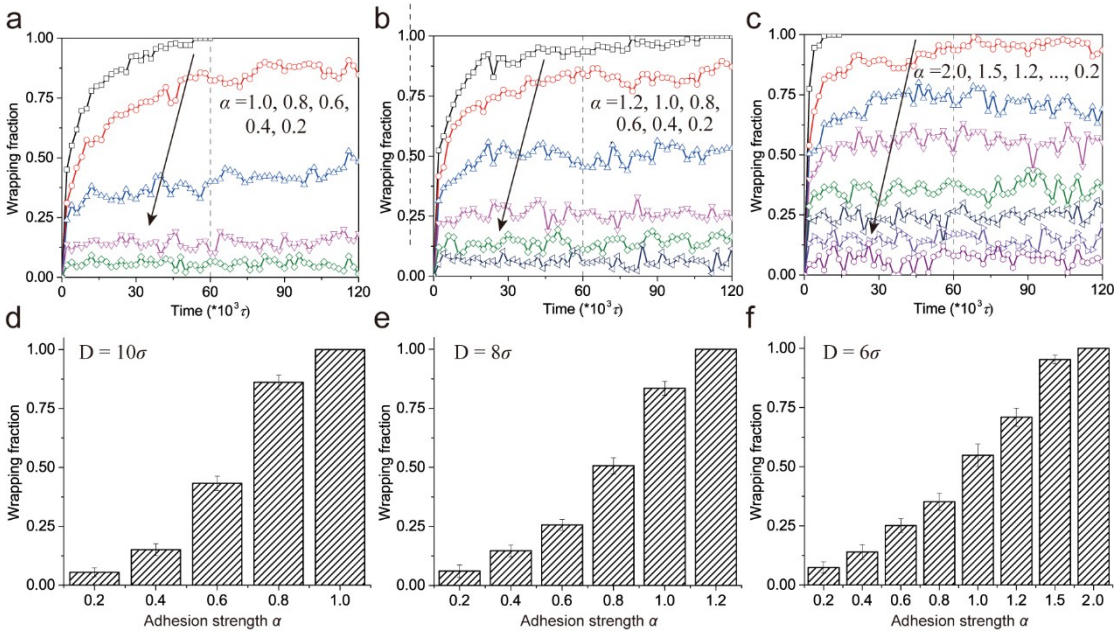

Fig. S2 Wrapping fractions of NPs as a function of adhesion strength α. (a), (b) and (c) are the evolution of the wrapping fractions of a single spherical NPs at different adhesion strength. (a), (b) and (c) are for NPs with diameters of 10σ, 8σ and 6σ, respectively. (d), (e) and (f) are the average wrapping fractions for NPs with diameters of 10σ, 8σ and 6σ, respectively.

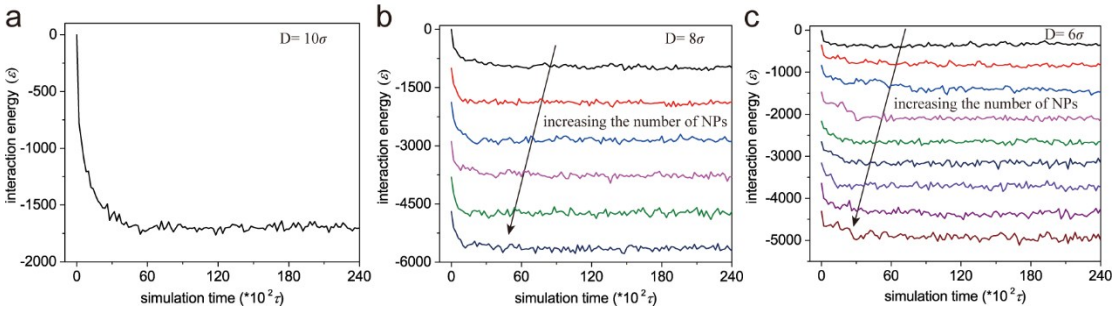

Fig. S3 The interaction energy between spherical NPs and the lipid membrane. (a), (b) and (c) are for spheres with diameters of 10σ, 8σ and 6σ. The arrows in (b) and (c) denote the interaction energy when more and more NPs are added to the system.

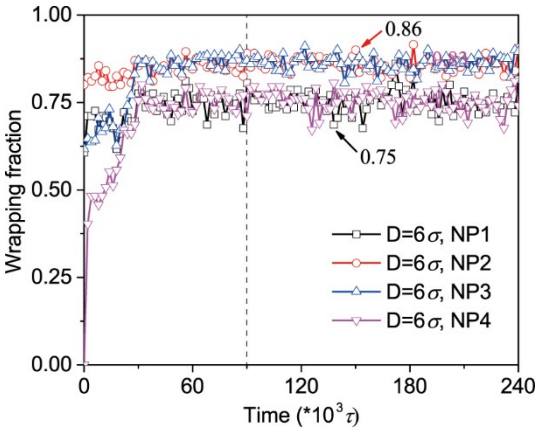

Fig. S4 Evolution of the wrapping fractions of spherical NPs when the fourth NP is added to the system. The numbers in the figures are the average wrapping fractions of NPs.

The hemifusion of lipid membrane mediated by spherical NPs

For spherical NPs with a diameter of 6σ, the NPs wrapped by the lipid membrane are approximately in the same plane, and the polygon formed by the centroids of these NPs are defined as Γ (Fig. S5a). For all lipids whose projections on the Γ-plane (Γ-plane is defined as the plane where the polygon Γ is located in.) are within Γ, we obtained the probability density of these lipid beads along the direction perpendicular to the Γ-plane (Fig. S5c). For prolate NPs (AR=3) with a D_v of 6σ, in which case the lipid membrane is neither fused nor hemifused (Fig. S5b), we also obtained the probability density of lipid beads, as show in Fig. S5d. For prolate NPs, the density of the second tail beads is close to zero near the Γ-plane, as indicated by the arrow in Fig. S5d, which is significantly lower than other positions. However, for spherical NPs, the density of the second tail beads near the Γ-plane is comparable to other positions, although it is a minimum. These results and the comparison confirm that the lipid membrane is hemi-fused for spherical NPs with a diameter of 6σ.

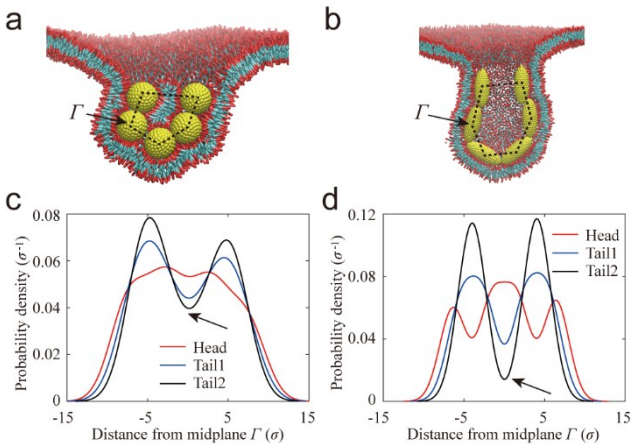

Fig. S5 The probability density of the lipid beads along the direction perpendicular to the Γ-plane. The polygon formed by the centroids of the NPs are defined as Γ, and Γ-plane is defined as the plane where the polygon Γ is located in. (a) and (c) are for spherical NPs with a diameter of 6σ. (b) and (d) are for prolate NPs with a D_v of 6σ. (a) and (b) are snapshots from our simulation and the illustrations of Γ. (c) and (d) are the probability density of the lipid beads.

Interaction of multiple spherical NPs with the lipid membrane

When the surface-to-surface distance between the two NPs is 10σ, the two NPs will approach each other and be wrapped together (Fig. S6a). When the distance is 20σ, each NP is individually wrapped by the lipid membrane (Fig. S6b). Meanwhile, the dynamics process of internalization for cooperative wrapping ($\sim 4000\tau$) is faster than individual wrapping ($\sim 5400\tau$).

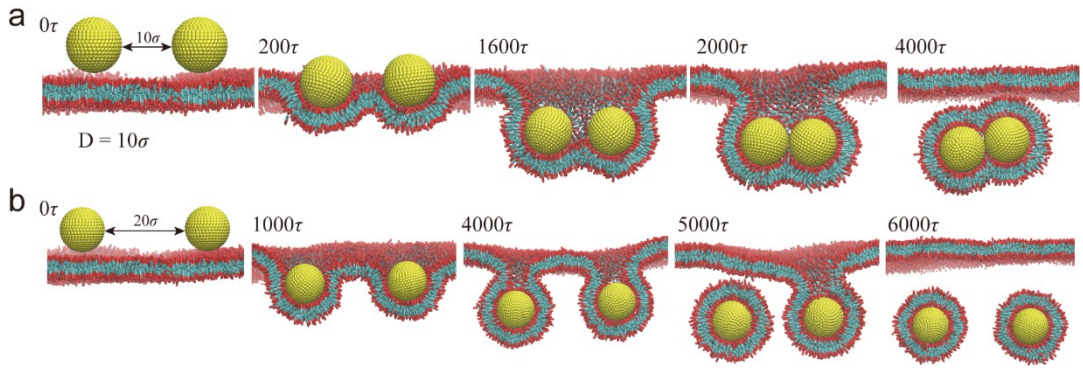

Fig. S6 Representative snapshots of the interaction between two spherical NPs ($D = 10\sigma$) and the lipid membrane. The surface-to-surface distance between the two NPs is (a) 10σ and (b) 20σ, respectively.

For small spherical NPs ($D = 8\sigma$), when four NPs are added to the system simultaneously, they can be completely wrapped by the membrane tube and detached from the membrane (Fig. S7a). When six NPs are added simultaneously, four of these

NPs are completely wrapped and detached from the membrane, the other two NPs are partially wrapped by the tubular membrane (Fig. S7b). When nine NPs are added simultaneously, the membrane will form two tubular structures to wrap these NPs, and one of the NPs even enter the other side of the membrane during the wrapping process (Fig. S7c). For smaller spherical NPs ($D = 6\sigma$), when four NPs are added simultaneously, the membrane forms a pocket-like structure to wrap these NPs, similar to the case when the NPs are added one by one (Fig. S7d). When six or nine NPs are added simultaneously, the membrane forms handle-like structure to wrap these NPs, in contrast to the pocket-like structure when the NPs are added one by one (Fig. S7e, S7f).

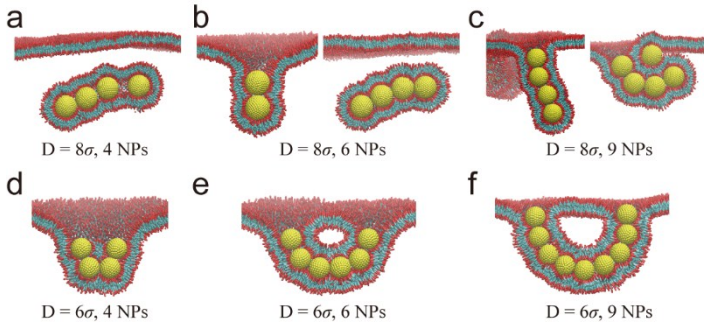

Fig. S7 Representative snapshots of the interaction between spherical NPs and the lipid membrane when multiple NPs are added to the system simultaneously. (a), (b) and (c) are the snapshots when four, six and nine spherical NPs with a diameter of 8σ are added, respectively. (d), (e) and (f) are for spherical NPs with a diameter of 6σ.

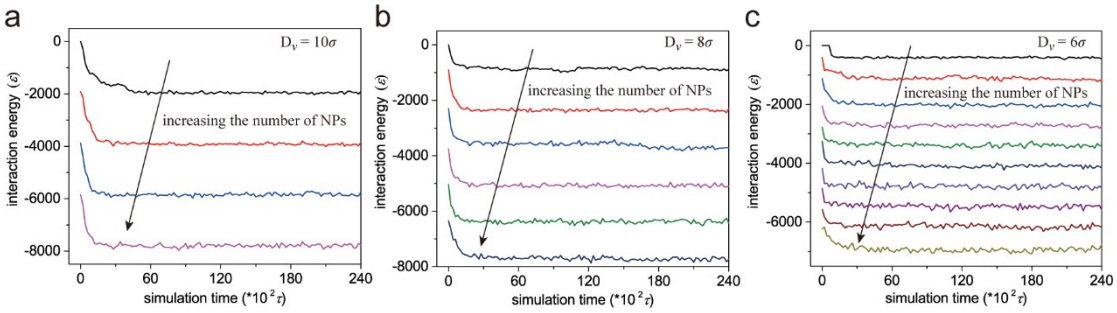

Fig. S8 The interaction energy between prolate NPs (AR=3) and the lipid membrane. (a), (b) and (c) are for prolate NPs with D_v values of 10σ, 8σ and 6σ. The arrows in (b) and (c) denote the interaction energy when more and more NPs are added to the system.

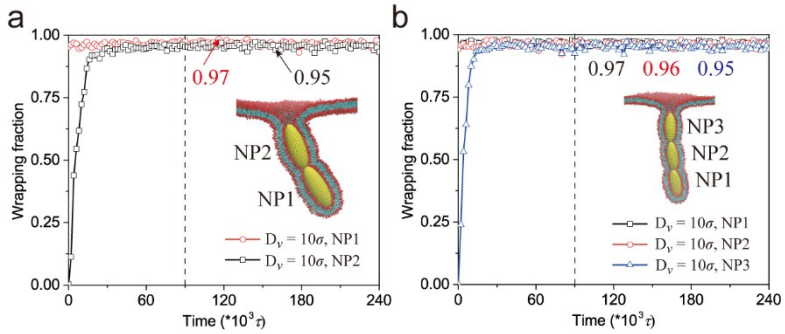

Fig. S9 (a) and (b) are evolution of the wrapping fractions of prolate NPs (AR=3 and $D_v = 10\sigma$) when the second and the third NPs are added to the system. The numbers in the figures are the average wrapping fractions of NPs.

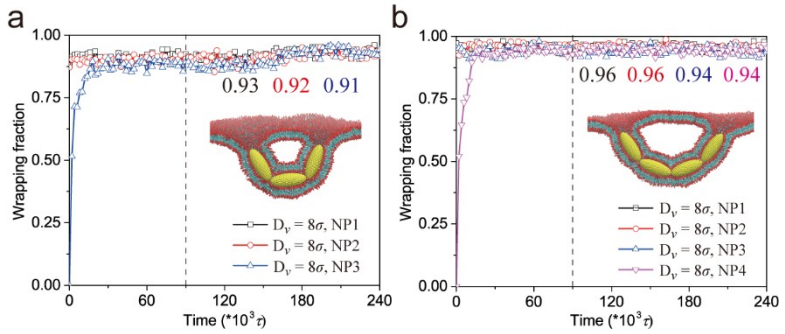

Fig. S10 (a) and (b) are evolution of the wrapping fractions of prolate NPs (AR=3 and $D_v = 8\sigma$) when the third and the fourth NPs are added to the system. The numbers in the figures are the average wrapping fractions of NPs.

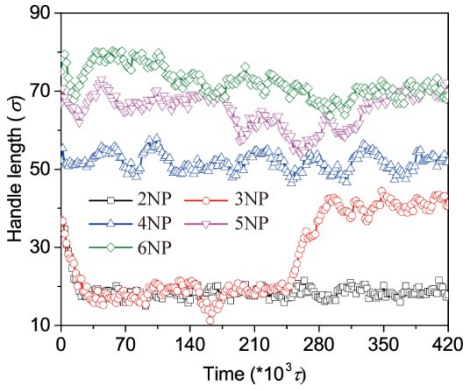

Fig. S11 Evolution of the handle-like structure length, L, as different numbers of NPs are filled in the handle. The handle length fluctuates significantly over time, for which we increase the simulation time to 4200000τ.

Wrapping the strongly curved tips of prolate NPs

The bending energy of the membrane would be significantly increased when the curvature radius of the membrane reaches the extent of the molecular length. In order

to test the extent to which the curvature of the lipid membrane can be achieved, we increased the adhesion strength α to 1.2, and studied the interaction between prolate NPs (AR=3) and lipid membrane (Fig. S12). For single prolate NPs with a D_v of 6σ, it is partially wrapped by the membrane (Fig. S12a). When the second NP is added, the membrane becomes disordered to wrap the two NPs, and some lipids escape from the membrane (Fig. S12b). It can be seen that it requires a large amount of adhesion energy to compensate for the energy cost of wrapping the strongly curved tips of the prolate NPs, and the wrapping may even damage the integrity of the membrane. Therefore, the partial wrapping state of small prolate NPs is common in our simulations.

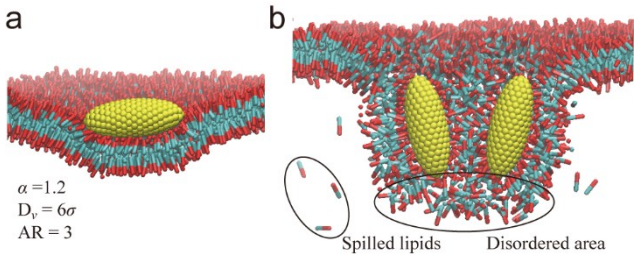

Fig. S12 Representative snapshots of the interaction between prolate NPs (AR=3, $D_v = 6\sigma$) and the lipid membrane. The interaction strength is set as $\alpha = 1.2$. (a) is for single NPs. When the second NP is added, the representative snapshot is shown in (b).

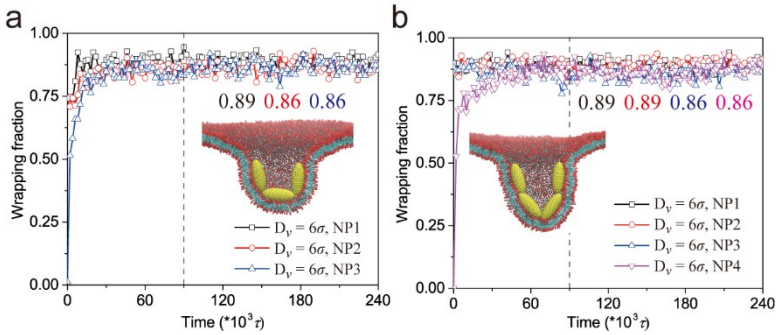

Fig. S13 (a) and (b) are evolution of the wrapping fractions of prolate NPs (AR=3 and $D_v = 6\sigma$) when the third and the fourth NPs are added to the system. The numbers in the figures are the average wrapping fractions of NPs.

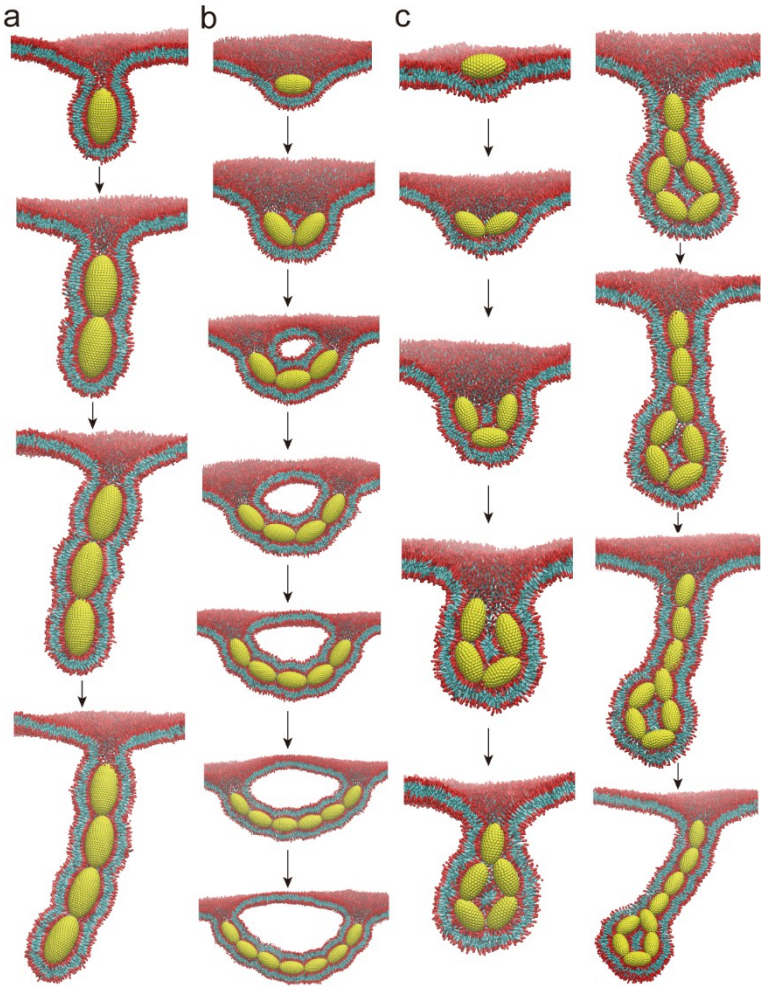

Fig. S14 Representative snapshots of the interaction between prolate NPs (AR=2) and the lipid membrane. (a) is for NPs with a D_v of 10σ. (b) and (c) are for NPs with D_v values of 8σ and 6σ.

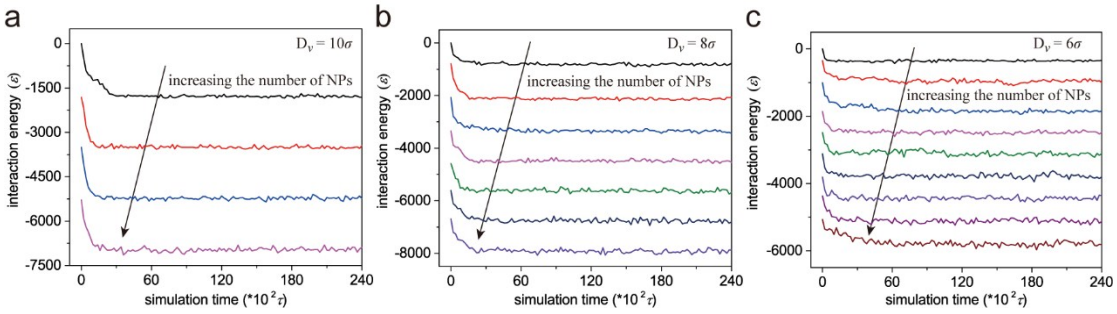

Fig. S15 The interaction energy between prolate NPs (AR=2) and the lipid membrane. (a), (b) and (c) are for prolate NPs with D_v values of 10σ, 8σ and 6σ. The arrows in (b) and (c) denote the interaction energy when more and more NPs are added to the system.

Interaction of multiple prolate NPs with the lipid membrane

We also study the case when multiple prolate NPs (AR=3) are added to the system simultaneously. For prolate NPs with a D_v of 8σ, the membrane forms pocket-like

structures to wrap multiple NPs (Fig. S16a-c). This is different from the observed handle-like structures when multiple prolate NPs ($D_v = 8\sigma$) are added to the system one by one. Thus, the order in which the NPs are added will affect the final NPs-membrane complex structure for these NPs. Meanwhile, these structures are all stable during our simulation time. For prolate NPs with a D_v of 6σ, the NPs-induced pocket-like membrane structures are substantially the same as those ones when NPs are added one by one (Fig. S16d-f).

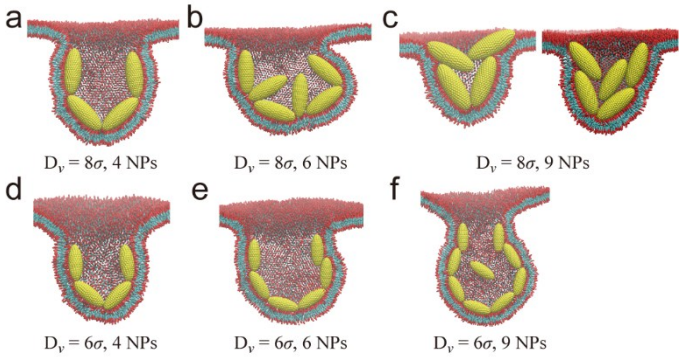

Fig. S16 Representative snapshots of the interaction between prolate NPs and the lipid membrane when multiple NPs are added to the system simultaneously. (a), (b) and (c) are the snapshots when four, six and nine prolate NPs with a D_v of 8σ are added, respectively. (d), (e) and (f) are for prolate NPs with a D_v of 6σ.

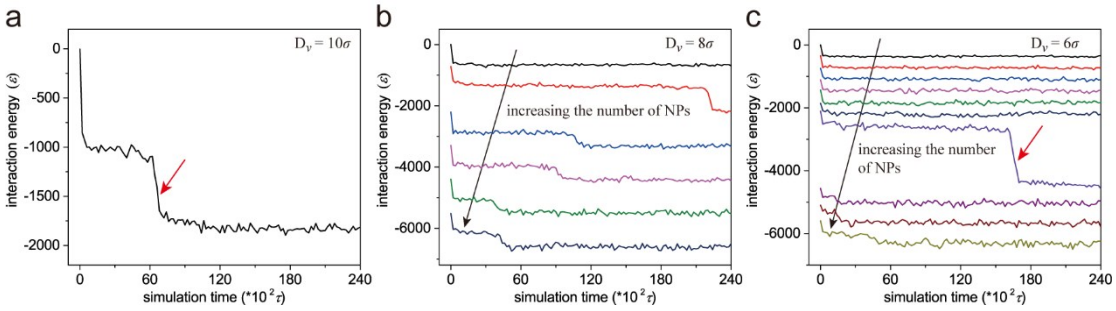

Fig. S17 The interaction energy between oblate NPs (AR=0.5) and the lipid membrane. (a), (b) and (c) are for oblate NPs with D_v values of 10σ, 8σ and 6σ. The black arrows in (b) and (c) denote the interaction energy when more and more NPs are added to the system. The red arrow in (a) shows the time at which the oblate NP change its orientation. The red arrow in (c) shows a sudden decrease in the interaction energy between the NPs and the membrane.

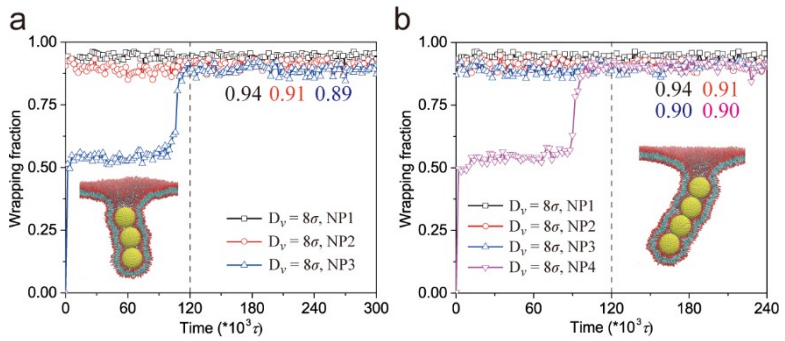

Fig. S18 (a) and (b) are evolution of the wrapping fractions of oblate NPs (AR=0.5 and $D_v = 8\sigma$) when the second and the third NPs are added to the system. The numbers in the figures are the average wrapping fractions of NPs.

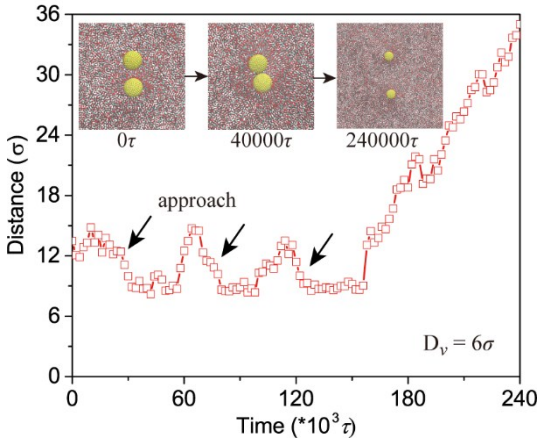

Fig. S19 Evolution of the distance between the two oblate NPs ($D_v = 6\sigma$). The two NPs approach each other several times and eventually leave each other (When the curved edges of the two NPs are attached together, the distance between them is 8.6σ). The insets are the snapshots show the distance of the NPs at different moments.

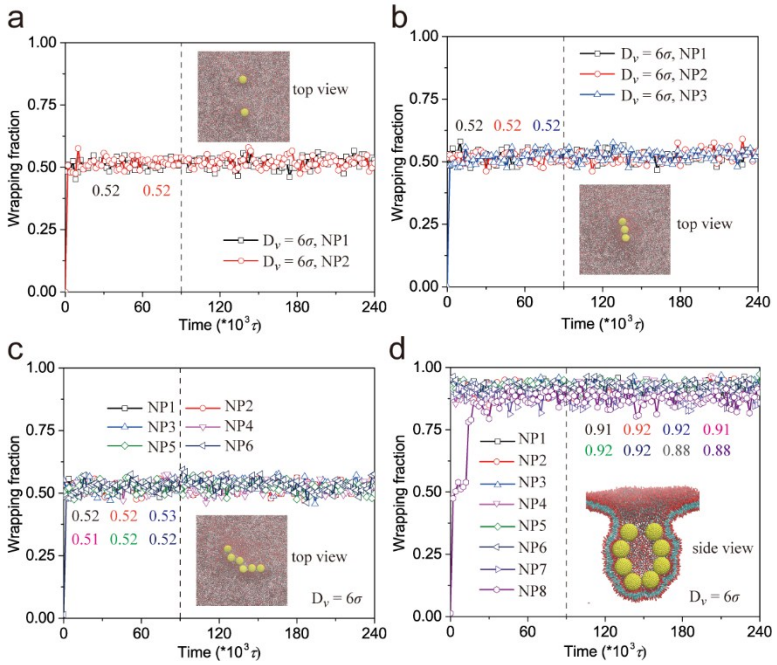

Fig. S20 Evolution of the wrapping fractions of oblate NPs (AR=0.5 and $D_v = 6\sigma$) when (a) the second, (b) the third, (c) the sixth, and (d) the eighth NPs are added to the system. The numbers in the figures are the average wrapping fractions of NPs.

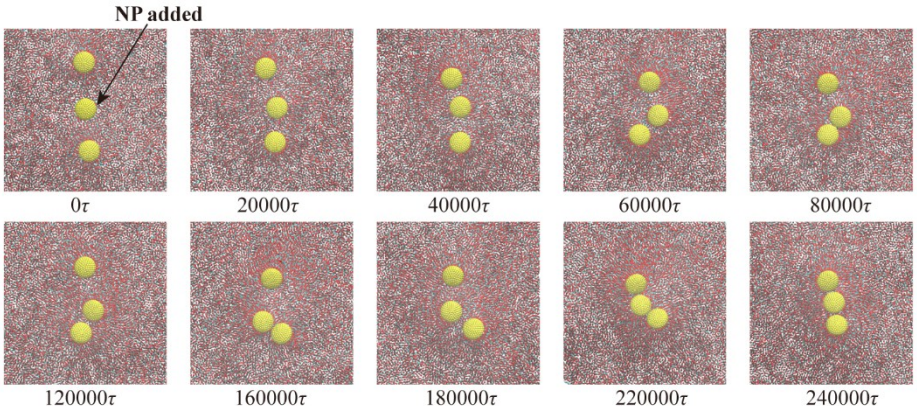

Fig. S21 Representative snapshots (top view) of the interaction between oblate NPs (AR=0.5, $D_v = 6\sigma$) and the lipid membrane when the third NP is added to the system.

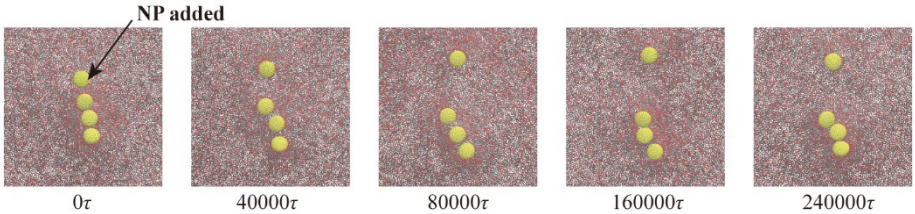

Fig. S22 Representative snapshots (top view) of the interaction between oblate NPs (AR=0.5, $D_v = 6\sigma$) and the lipid membrane when the fourth NP is added to the system.

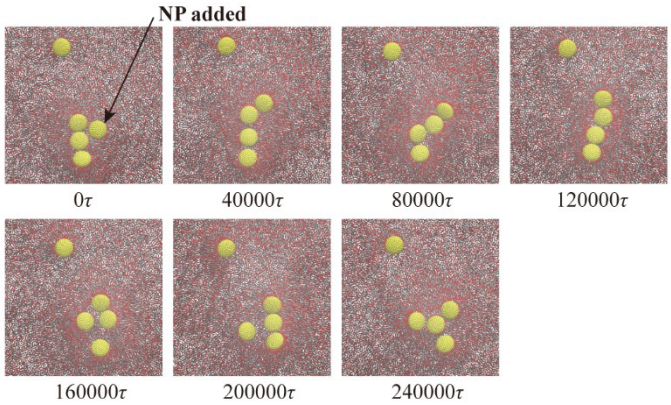

Fig. S23 Representative snapshots (top view) of the interaction between oblate NPs (AR=0.5, $D_v = 6\sigma$) and the lipid membrane when the fifth NP is added to the system.

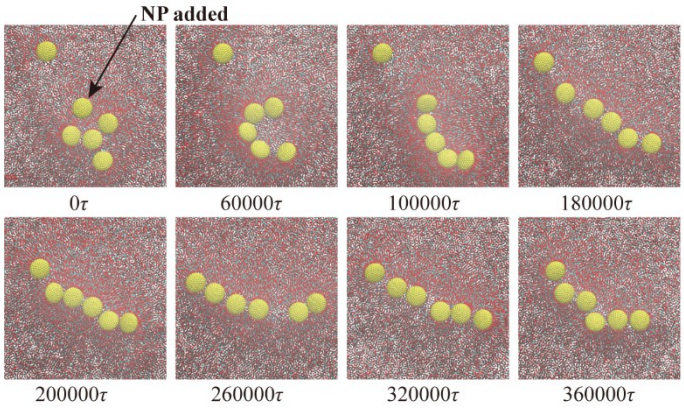

Fig. S24 Representative snapshots (top view) of the interaction between oblate NPs (AR=0.5, $D_v = 6\sigma$) and the lipid membrane when the sixth NP is added to the system.

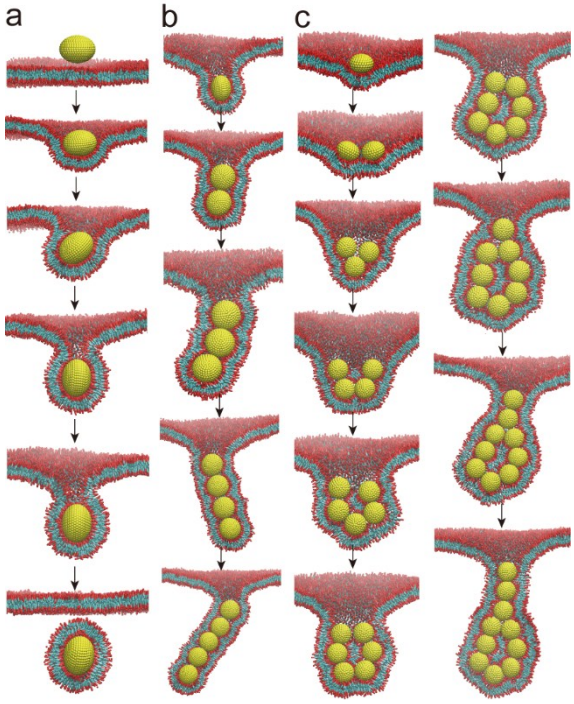

Fig. S25 Representative snapshots of the interaction between oblate NPs (AR=0.75) and the lipid membrane. (a) is for NPs with a D_v of 10σ. (b) and (c) are for NPs with D_v values of 8σ and 6σ.

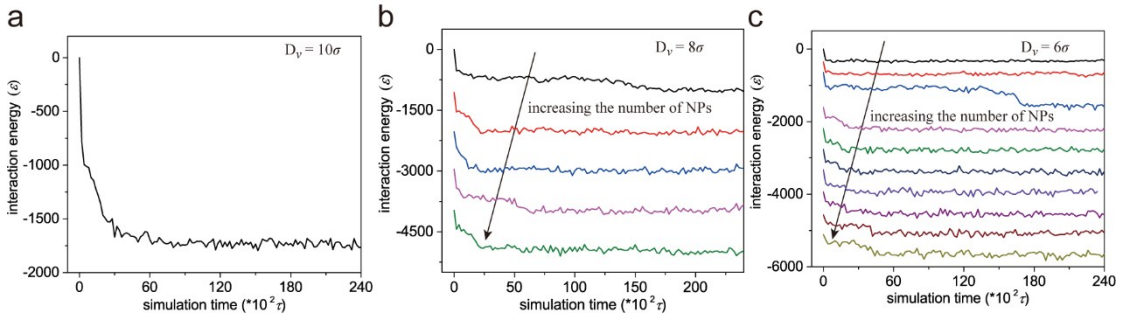

Fig. S26 The interaction energy between oblate NPs (AR=0.75) and the lipid membrane. (a), (b) and (c) are for oblate NPs with D_v values of 10σ, 8σ and 6σ. The arrows in (b) and (c) denote the interaction energy when more and more NPs are added to the system.

Interaction of multiple oblate NPs with the lipid membrane

For oblate NPs with a D_v of 8σ, the membrane also forms pocket-like structures to wrap multiple NPs (Fig. S27a-c), which contrasts with the tubular structures when NPs are added one by one. For oblate NPs with a D_v of 6σ, the NPs-induced pocket-like membrane structures are similar with the ones when NPs are added one by one (Fig. S27d-f).

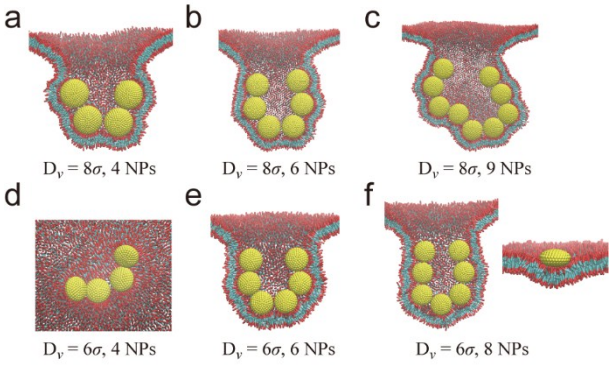

Fig. S27 Representative snapshots of the interaction between oblate NPs and the lipid membrane when multiple NPs are added to the system simultaneously. (a), (b) and (c) are the snapshots when four, six and nine oblate NPs with a D_v of 8σ are added, respectively. (d), (e) and (f) are for oblate NPs with a D_v of 6σ.

Video_S1.m2v

Video S1: The interaction between oblate NPs (AR=0.5, $D_v = 6\sigma$) and the lipid membrane when the seventh NP is added to the system.

1. I. R. Cooke and M. Deserno, *J. Chem. Phys.*, 2005, **123**, 224710.
2. I. R. Cooke, K. Kremer and M. Deserno, *Phys. Rev. E*, 2005, **72**, 011506.
3. M. Simunovic and G. A. Voth, *Nature Communications*, 2015, **6**, 7219.